1. Introduction

1.1 General Purpose

This thesis presents a multiscale examination of low-level flow channeling in the Mohawk and Hudson River valleys of New York State. Insight into how synoptic and mesoscale flow patterns interact with the region's topography to drive low-level flow convergence (known colloquially as Mohawk–Hudson convergence and, hereafter, as MHC) is obtained by examining several detailed case studies. Case-to-case similarities prior to and during MHC events are described in an effort to develop an operational forecasting strategy.

The remainder of this chapter will provide a literature review of pressure-gradient-driven flow channeling, with an emphasis on orographic channeling of low-level flow. An examination of orographically induced low-level convergence zones is included, such as the Puget Sound convergence zone, the Snake River Plain convergence zone, and the Denver Cyclone. Several existing studies of how orographic features in eastern New York and western New England impact the local climatology will also be presented. This chapter ends with a discussion of the scientific goals and organizational structure of this thesis.

1.2 Review of Available Literature Discussing Orographically Modified Flows

The literature review begins by discussing the basic conditions which favor orographically altered valley wind flows and the means by which they are produced. Examples of the influence that low-level flow channeling within a valley has on the precipitation distribution are introduced next. Finally, existing research on how the

Mohawk and Hudson valleys influence the weather of eastern New York and western New England, specifically during the warm season, is highlighted.

1.2.1 The Basics of Low-Level Flow Channeling Within a Valley

Flow channeling occurs when orographic features, such as breaks in mountain barriers or valleys through hilly terrain, act to change the local wind direction or speed. Oftentimes this phenomenon reveals itself as a recurring area of surface wind observations that differ systematically from surrounding observations, and which occur only under certain specific synoptic conditions.

Intuitively, one might imagine that only highly exaggerated terrain or deep valleys would effectively channel winds, but Gross and Wippermann (1987) prove otherwise in their examination of channeling in Germany's upper Rhine valley. The authors indicate that the broad and flat valley, which has a width of only 35 km and is flanked by mountains on each side that rise only about 500 m, is nevertheless an effective flow channeling mechanism (Fig. 1.1a; Gross and Wippermann 1987). The Hudson valley of New York, which is approximately 45 km wide and is flanked by terrain that rises no more than 750 m above the valley floor (a measurement known hereafter as "local relief"), is similar in scale to the upper Rhine valley and would therefore likely be an effective flow-channeling mechanism (Fig. 1.2). The hourglass shape of the Mohawk valley, which comprises two broad plains (one located near Rome, NY; the other near Albany, NY) funneling into a relatively narrow (approximately 15-km wide) section, and local relief similar to that of the Hudson valley, also points to the Mohawk's effectiveness for flow channeling, following Gross and Wippermann (Fig. 1.2).

In their treatment of the relatively broad and shallow Tennessee valley (Fig. 1.1c) Whiteman and Doran (1993) examined four mechanisms that can produce valley winds that differ from the overlying winds found above the valley. The first process, thermal forcing, produces strong day-to-night shifts in wind direction within the valley and is not prone to occur in shallow valleys (Whiteman and Doran 1993). As both the Hudson and Mohawk valleys are characterized as shallow in the framework of Gross and Wippermann (1987), and as no discernable diurnal wind signature appears with respect to them, thermal forcing is not expected to affect winds within these valleys to any great extent. The downward transport of horizontal momentum from above a valley is the second process that can influence winds within a valley, according to Whiteman and Doran (1993). This process generates in-valley winds that are of a similar direction as the overlying, ambient flow. In most instances where MHC is occurring, it will be shown that a low- to mid-level temperature inversion is present and that surface winds within the valleys tend to be light (less than 8 m s^{-1}), indicating that downward momentum transfer is relatively unimportant. Winds within a valley can oppose the direction of the ambient flow if the third process presented by Whiteman and Doran (1993), known as "forced channeling," is at work. This process directs the perpendicular (relative to the valley) component of the overlying geostrophically balanced winds into the valley, in a direction that is parallel to the valley axis. Occasional but sudden changes in direction can occur when overlying geostrophic winds become more- or less-normal to the valley sidewalls. Wind directions prior to, during, and following MHC events, conversely, shift subtly and gradually, indicating that forced channeling likely plays little or no role. Finally, Whiteman and Doran (1993) assert that valley winds can arise from the geostrophic pressure gradient that is aligned along the valley's axis. This final process is called "pressure-driven channeling." Gross and Wippermann (1987) also addressed this phenomenon, stating that pressure-driven channeling is produced when a column of air passes across a valley and expands vertically, becoming subgeostrophic and turning left, referenced to the direction of the large-scale pressure gradient (Fig. 1.3). In this way, only the along-valley component of the large-scale pressure gradient is effective in driving the winds within a valley (Gross and Wippermann 1987). Whiteman and Doran (1993) argue that it is the pressure gradient directed along the valley alone that affects valley winds, and that air is not necessarily required to expand into the valley from above, stating that:

> "Pressure-driven channeling is expected to be a dominant mechanism in valleys under conditions where the influence of the downward momentum transport and thermal wind mechanisms are minimized. This occurs for shallow, but well-channeled, linear valleys in a climatological regime with light to moderate geostrophic above-valley winds and slightly or moderately stable atmospheres."

The authors go on to state that "[t]o date, the pressure-driven channeling mechanism has been documented for Germany's Rhine Valley and in the Tennessee Valley" (Whiteman and Doran 1993). The Mohawk and Hudson valleys are also shallow, well-channeled, linear valleys, and it will be shown that all MHC cases examined occur in light to moderate geostrophic flow regimes, with a high overall static stability in the lower troposphere. It follows, then, that pressure-driven channeling may be a dominant force in the formation of MHC.

Kossmann and Sturman (2003) continue the discussion of pressure-driven channeling, asserting that the wind speed generated within a valley is proportional to the pressure gradient force (PGF) that acts along the valley axis. They note that a greater frequency of channeling events is seen in the presence of more stable atmospheric stratifications, which act to decouple winds within a valley from the ridge-level winds and limit downward mixing of momentum from above (Kossmann and Sturman 2003).

Kossmann and Sturman (2003) also dissect pressure-driven channeling within a curved or bent valley, where the angle between the synoptic-scale pressure gradient vector and the valley axis will differ from one valley segment to another. The Mohawk and Hudson valleys, while themselves linear in nature, intersect near Albany, NY (KALB), at an approximate 100° angle, which may generate effects similar to those caused by a valley bend. Following Kossmann and Sturman (2003), and given this valley configuration and the typical background PGF associated with MHC, Fig. 1.4h mostly closely approximates how the valleys and the effects of pressure-driven channeling interact. In this configuration, the along-valley PGF is of the same sign in both valleys but of greater magnitude along the Mohawk valley, resulting in convergence at the valley bend and associated upward vertical motion. This bent-valley effect could contribute to the surface convergence that gives rise to MHC, although it is likely not the primary cause. Kossmann and Sturman (2003) go on to say that inertial effects, owing to differing wind speeds in each segment of a bent valley, can displace the convergence zone away from the valley bend and in the direction of the stronger wind speed. In the case of MHC, precipitation is rarely centered directly over the intersection of the Mohawk and Hudson valleys, and its actual location may be modulated by the aforementioned inertial effects.

1.2.2 Effects of Low-Level Flow Channeling on Precipitation

The orographic channeling of low-level winds can impact the precipitation distribution in several ways. In some cases, channeled flow can modify the temperature profile of the atmosphere enough to locally change the phase of falling precipitation. Orographic channeling of low-level flow may also lead to zones of convergence, which can in turn generate areas of mesoscale precipitation. The Puget Sound of Washington State, the area surrounding Denver, Colorado, and the Snake River Plain of eastern Idaho are among the areas that experience precipitation from these convergence zones.

1.2.2.1 PUGET SOUND CONVERGENCE ZONE

Chien and Mass (1997) introduce the Puget Sound convergence (PSCZ) as "probably the most important topographically induced mesoscale phenomenon affecting the Puget Sound lowlands." In a given year, the PSCZ occurs dozens of times and has a significant impact on the climatology of the region (Chien and Mass 1997). Whitney et al. (1993) indicate that "the PSCZ can be strong enough to produce thunderstorms with brief heavy rain, snow, ice pellets or hail," and that, during the cold season, can produce over 100 cm of snow per event, necessitating winter storm warnings. While MHC does not appear to have a discernable effect on the climate of eastern New York and western New England, its evolution does share some similarities with the PSCZ and its impacts on the public can be significant several days per year.

A conceptual model of the PSCZ, presented by Mass (1981), illustrates the way in which the Cascade Mountains, Strait of Juan de Fuca, and Chehalis Gap act to direct northwest low-level flow off of the Pacific Ocean and over the Puget Sound, forming a convergence zone, and creating enhanced precipitation around Seattle and Everett (Fig. 1.5). These conditions (and the resulting convergence zone) are shown by Mass (1981) to be most likely during the late spring and early summer months due to the wind climatology of the region. Chien and Mass (1997) also note that PSCZ events tend to develop directly following a cold frontal passage. This postfrontal environment is also characteristic of MHC development, which also shows a strong seasonal dependence.

Utilizing sets of case studies selected at random, Mass (1981) finds that the PSCZ develops only through a narrow subset of coastal surface wind directions, as measured at several representative sites (Fig. 1.6). Winds are generally of light or moderate speeds (approximately 2.5–7.5 m s^{-1}), and several calm readings are reported in the area of surface convergence during PSCZ events (Mass 1981). A similarly narrow range of surface wind directions are present at bellwether sites during MHC and wind speeds are generally light to moderate as well, as shown in Table I.

A case and subsequent modeling study of a PSCZ even that occurred on 26 May 1992 is presented by Chien and Mass (1997) and provides insight into what drives the PSCZ phenomenon. Initially, surface winds in the convergence zone were quite weak (and, at times, calm), and throughout the entire event analyzed wind speeds were 5 m s^{-1} or less (Fig. 2, not shown; Chien and Mass 1997). These light-to-moderate wind speeds are characteristic of those present during MHC events as well.

Chien and Mass (1997) found that the PSCZ could be modeled successfully by the Pennsylvania State University–National Center for Atmospheric Research Mesoscale Model (PSU–NCAR MM5), and determined that both the Olympic and Cascade Mountains are critical to the formation of the convergence zone (Fig. 1.7). These terrain features act to steer the onshore flow so that this flow splits and then converges over the central Puget Sound; without these features and the split flow, the PSCZ does not form (Chien and Mass 1997). Furthermore, the modeling of this event corroborates what Mass (1981) had found previously through examining vertical wind profiles; namely, the winds responsible for PSCZ formation are relatively shallow with a depth generally less than 1.2 km. It should be noted that the winds responsible for producing MHC are even shallower, on the order of 0.5 km in depth.

Additional model results indicate that, during its strongest phase, the PSCZ produces maximum vertical motions centered at approximately 850 hPa (Chien and Mass 1997; Figs. 1.8 and 1.9). It will be shown that maximum vertical motions associated with MHC tend to be centered lower in the atmosphere (around 925 hPa) and are weaker, even during the peak of events.

Modeling conducted by Chien and Mass (1997) also reveals the important role that latent heat release plays in regard to the formation and strength of the PSCZ. Latent heat released by condensation in the rising air acts to destabilize the lower troposphere, creating a positive-feedback mechanism in which convection and accompanying low-level convergence strengthens. The removal of latent heating from the model simulations of the 26 May 1992 case still allowed the PSCZ to form, but in a weakened state. Without latent heat effects, “low-level wind convergence near the central [Puget] sound is attenuated compared to the control run; in addition, there is lighter and more widespread precipitation over the Puget Sound” due to greater stability, which limits vertical development (Chien and Mass 1997). It will be shown that, with precipitable water (PWAT) values between 3.8 and 7.6 mm and high static stability present in all cases, MHC lacks the contribution of latent heat release. This key difference likely explains the shallow nature of ascent and precipitation associated with MHC, and plays a substantial role in limiting its overall climatological impact.

Mass (1981) experimented with forecasting the PSCZ through examining synoptic-scale weather features. The experiments resulted in a successful prediction of the PSCZ 22 out of 23 times, but also indicated several "false alarm" events which did not actually occur (Mass 1981; Fig 1.10). Overall, Mass (1981) found that the PSCZ is inherently predictable, given accurate forecasts of surface wind speed and direction. Building on this finding, Whitney et al. (1993) conclude that "it is possible to make a reasonably skillful medium-range forecast of the occurrence of a PSCZ." To that end, a methodology and decision tree for forecasting the PSCZ was devised (Fig. 1.11), and was put into operational use by the Seattle Forecast Office of the National Weather Service. Whitney et al. (1993) highlight the important role that coastal surface wind direction plays in allowing the PSCZ to form by making it the first criterion of the decision tree. When the direction and speed of surface winds at Hoquium, Washington (KHQM), fall into a predetermined range, a PSCZ event is likely within several hours. Furthermore, the likelihood of PSCZ formation increases as the initially larger west-to-east sea-level pressure (SLP) difference becomes similar in magnitude to the north-to-south SLP. Such a rotation of the SLP gradient permits a generally southwest and west-southwest surface flow to develop over western Washington State. As this southwest and west-southwest flow develops it can sometimes bifurcate around the Olympic Peninsula, with one part of the flow moving down the Strait of Juan de Fuca and turning southward across Puget Sound and the other part of the flow moving across the Puget Sound lowlands and turning northward across Puget Sound. Where the northerly and southerly air streams in Puget Sound converge marks the location of the PSCZ.

Whitney et al. (1993) conclude that the only factors controlling lead time for PSCZ forecasts are the accuracy of model simulations and forecaster confidence. Like the PSCZ, MHC is a mesoscale phenomenon driven by synoptic-scale features and likely has a high degree of predictability in the medium- to short-range.

1.2.2.2 Snake River Plain Convergence Zone

Andretta and Hazen (1998) describe the Snake River Plain convergence zone (SRPCZ) as a periodic feature that forms in the Snake River Plain (SRP) of eastern Idaho under northwest synoptic flow at mid and low levels. Fig. 1.12 reveals that the SRP is approximately 100 km wide and features local height relief of 1700 m with respect to the bounding mountains to the northwest, and 400 m with respect to the bounding mountains to the southeast (Andretta and Hazen 1998). The valley-to-ridgeline height difference to the southeast is somewhat similar to that of the Mohawk or Hudson valleys but, overall, local relief is much greater in the case of the SRP.

Steenburgh and Blazek (2001) highlight the effectiveness of the SRP in channeling low-level flow through their study of a cold front that was distorted by the topography of the region. Fig. 1.13 shows the progression of the cold front through the SRP and an accompanying frontal bulge, which developed as the cold front was locally accelerated within the SRP. The acceleration is attributed by Steenburgh and Blazek (2001) to an isolated wind maximum that developed directly behind the cold front within the plain. The authors go on to explain that the development of this wind maximum is a direct result of the highly ageostrophic flow field that developed within the channeled terrain.

Andretta and Hazen (1998) present a case study of a SRPCZ event that took place on 26 November 1995 and was preceded by the passage of a surface cold front. This front brought an end to synoptic-scale precipitation and was associated with a 40 m decrease in the 1000–500 hPa thickness over 6 h, indicating cold advection. Behind the front, the rise in SLP pressure averaged 4 hPa as the pressure gradient in the area tightened significantly. Geopotential height rises and a tightening of the geopotential height gradient accompanied weak cyclonic flow at 850 and 700 hPa. Also, the static stability of the lower troposphere decreased, with lapse rates increasing from 5.7 to 7.0°C km^{-1} over 7 h. Aside from the presence of low-level cold advection, which is characteristic of MHC, there are few similarities between the synoptic patterns associated with MHC and SRPCZ. Steady, rising, and falling SLP trends are all observed during MHC events, and neutral or falling heights are observed at 850 and 700 hPa. In many cases, cyclonic curvature of the 850- and 700-hPa geopotential height contours is present during MHC events, but such curvature is not always pronounced.

Using the Weather Surveillance Radar-1988 Doppler (WSR-88D) located in Springfield, Idaho (SFX; see Fig. 1.12 for location), and various surface observation sites, Andretta and Hazen (1998) diagnose mesoscale wind patterns throughout the SRPCZ event of 26 November 1995. At the onset, the lowest tilt of the radar (at a 0.5° elevation above horizontal, or slightly above the 850-hPa level given the elevation of the radar site) reveals the presence of 16–21 m s^{-1} winds as well as a band of moderate-to-heavy snow (24–44 dBZ) over the region. Surface winds [as indicated by mesoscale observation network (mesonet) sites] of 5–15 m s^{-1} are also present. A convergent wind signature seen over the upper SRP in the lowest 1 km of the atmosphere on the radar's Vertical Azimuth Display (VAD; not shown) is attributed to the SRPCZ, and a zone of low-level convergence. This zone and an attendant area of precipitation associated with 35–45 d*BZ* radar reflectivities propagate down-valley at approximately 5–10 m s^{-1}. Maximum snowfall totals from the SRPCZ event ranged from approximately 10.2 to 15.3 cm. Qualitative similarities between the MHC and the SRPCZ exist, including the vertical stratification of winds, the relatively shallow atmospheric depth of convergence, and the propagation of convergence zone, but quantitative differences also exist. These differences include wind speeds, both at the surface and aloft (which are generally half as great during MHC events), depth of convergence (again, half as great during MHC events), and precipitation intensity (which generally does not exceed 30 d*BZ* in cases of MHC).

1.2.2.3 Denver Cyclone

In their seminal paper, Szoke et al. (1984) describe the formation of a narrow line of surface convergence and cyclonic turning of low-level winds in the vicinity of Denver, Colorado, which they dubbed the Denver convergence–vorticity zone (see Fig. 1.14). Also known as the Denver Cyclone (DC) in several subsequent papers (e.g., Wilczak and Glendening 1988; Wilczak and Christian 1990), Szoke et al. (1984) came upon the phenomenon while investigating the 3 June 1981 tornado outbreak in the Denver area, the worst tornadic outbreak for the region to date at that time. Identifying the presence of the convergence–vorticity zone more than 5 h before the tornado outbreak, Szoke et al.

(1984) note its importance in the development of severe weather that day, and acknowledged the role that this mesoscale feature may have played in tornado spin-up. The authors briefly examine two seasons (May–August of 1981–82) of severe weather occurrences in the Denver area, finding a correlation between a convergence–vorticity zone regime and the occurrence of severe weather. Namely, they find that during the period of study 14 out of the 23 reported tornadoes (61%) occurred in the presence of a convergence–vorticity zone (which may or may not include a closed circulation), or in the presence of south to southeasterly surface flow.

The topography of the north-to-south oriented Rocky Mountain Front Range features significantly more local relief than that of eastern New York and western New England, with peak elevations of more than 3700 m in northeastern Colorado and a 2000 m rise occurring in less than 20 km (Wilczak and Glendening 1988; Fig. 1, not shown). The DC itself occurs in the lee of the Front Range, bounded by two west-to-east oriented ridges: the Cheyenne Ridge to the north and the Palmer Ridge to the south.

Case studies of two different DC events provide insight into its life cycle and manifestation. In their treatment of the DC event of 1 August 1985, Wilczak and Glendening (1988) show that the gyre develops following the passage of a surface cold front, in an air mass that becomes more stably stratified with time. A southeasterly surface return flow sets up several days later, allowing a well-mixed boundary layer to grow slowly out of a stable layer, which was initially present from the surface to a height of about 1 km above ground level. The authors also find falling pressures in the vicinity of the mature gyre. In most instances of MHC, which also tend to follow the arrival of a cooler and more stably stratified airmass, surface pressures tend to be nearly steady or rising during the mature phase.

A case study by Wilczak and Christian (1990) of a DC occurrence, which began on 25 June 1987 and persisted in a quasi-steady-state fashion for 30 h, indicates that this feature developed in the presence of a stable nocturnal inversion layer (their Fig. 4, not shown). Beginning under weak upper-level synoptic forcing as a shallow, near-surface phenomenon (as revealed in wind reports gathered from observation towers and wind profilers), the mixed layer and vortex both grew in depth over the next several hours to a height at which a strong inversion layer existed, i.e., 700 hPa. As ground level in the vicinity of Denver occurs at approximately 850 hPa, this height indicates that the DC occurred only in the lowest 150 hPa of the atmosphere, the depth of which is similar to MHC. It will be shown that the discernable wind and model-diagnosed vertical-motion signatures associated with MHC generally occur only in the lowest 75 hPa of the atmosphere.

Wilczak and Christian (1990) also examined how the presence of the DC may have assisted in the formation of severe thunderstorms during the 25 June 1987 episode. The close inspection by these authors of radar data showed weak cells (reflectivities less than 25 dBZ) forming over the mountains to the west of Denver, which dissipated as they drifted eastward. Some of these dissipating elevated cells passed over part of the convergence zone associated with the DC and reached 40 dBZ in intensity within an hour doing so, while the strongest cells reached 70 dBZ, split, and produced hail up to 4.5 cm in diameter. From the timing of the supercells' formation, the authors infer that the dissipating elevated cells may have triggered convection along the convergence zone as they passed overhead. This inference suggests a mechanism by which existing precipitation can be enhanced by the presence of a convergence zone, a mechanism that will be discussed later in reference to MHC.

Through their mixed-layer modeling of the 1 August 1985 DC episode, Wilczak and Glendening (1988) conclude that "baroclinicity is of paramount importance in the formation of the Denver Cyclone." Conversely, close inspection of multiple MHC events indicate that baroclinicity is not a factor in the formation of MHC. Furthermore, the presence of large amounts of baroclinicity may, in fact, inhibit MHC from forming, as the stronger forcing generally associated with baroclinic regimes would tend to overpower the weaker pressure-driven forcing which accompanies MHC.

1.2.2.4 Longmont Anticyclone

The Longmont Anticyclone (LA) is introduced by Wesley et al. (1995) as a counterpart of the Denver Cyclone, stating "[t]he Longmont Anticyclone [is] a region of low-level anticyclonic turning and convergence," which forms when northerly flow along the Front Range of the Rocky Mountains interacts with the complex local terrain (Fig. 1.15). The LA forms in a post frontal environment (similar to the phenomena previously discussed above, including MHC), as a gusty, partially isallobaric wind develops in response to rapid surface pressure rises over Wyoming. The low-level northerly flow turns anticyclonically and decelerates in the lee of the Cheyenne Ridge (the axis of which is seen just north of the Colorado–Wyoming border in Fig. 1.15), and the resulting convergence can generate precipitation. The ensuing precipitation can have a significant impact on local snowfall distributions, despite the shallow, anticyclonic nature of the air mass (Wesley et al. 1995). The authors also note that preexisting precipitation that enters the area can be enhanced by an ongoing LA, an effect that will be further examined with regard to MHC.

In their case study of the LA event of 16 January 1991, Wesley et al. (1995) documented a synoptic environment which is strikingly similar to that of MHC events The synoptic environment included: 1) the lack of any jet streak dynamics; 2) the presence of a large-scale 500 hPa trough with northwest flow and slowly falling geopotential heights; 3) the lack of robust vorticity advection; 4) weak low-level cold advection following the passage of a weak surface cold front; 5) a period of calm surface winds in the area of convergence; and 6) low-level winds generally weaker than 10 m s^{-1} during the event. As determined by vertical thermodynamic and wind profiles taken in the region at the onset of the 16 January 1991 LA event (not shown), the atmosphere was moist from the surface to 500 hPa and featured a shallow, ground-based stable layer, above which dry-adiabatic lapse rates existed to 690 hPa. It should be noted that the Appendix of Wesley et al. (1995) addresses the unusual nature of saturated atmospheric conditions coexisting with dry-adiabatic lapse rates, and the way in which riming on humidity sensors may have caused inaccurate measurements. Ultimately, though, the authors conclude that relative humidities above 75% were present in the 800–600 hPa layer. At the peak of the LA, a moist and conditionally unstable layer was found in the lowest 130 hPa of the atmosphere, with a layer of greater static stability (and moist-adiabatic lapse rates) above. The stabilization of the lower troposphere, warming of cloud top temperatures (CTTs), and drying in the low and midlevels of the atmosphere coincided with the end of the LA event. The thermodynamic profile presented by Wesley et al. (1995) indicates that the atmosphere was supportive of convection throughout much of the LA event, a contrast to the stably stratified atmosphere common to MHC cases. The vertical wind profiles also speak to the shallow nature of the LA (another characteristic shared by MHC), with Wesley et al. (1995) detecting the wind signature associated with the LA in a layer only 500 m deep.

Radar loops of the precipitation intensity associated with the LA event of 16 January 1991 indicate that intensification of weaker echoes occurred as they moved from north-to-south through the convergence zone domain (Wesley et al. 1995). Radar reflectivity values as high as 30 dBZ were noted as snowbands drifted across the area where the LA was present, with heavy snow and wind gusts to 9 m s^{-1} reported as one such band passed the Denver observation site. Snowfall amounts totaled 6–9 cm just south of the LA region (over and west of DEN and BOU, Fig. 1.15), and was attributed by Wesley et al. (1995) to convergence. It will be shown that the amount of snow that falls during typical MHC events, and the corresponding radar reflectivities, are on the order of what fell during the LA event discussed by Wesley et al. (1995).

1.2.2.5 Cold-Air Damming in the Appalachian Mountains

Citing Richwein (1980), Bell and Bosart (1988) define cold-air damming (CAD) as "[t]he phenomenon of cold air becoming entrenched along the slopes of mountain ranges..." Utilizing archived surface weather charts, Bell and Bosart (1988) developed a monthly climatology of CAD events along the eastern slopes of the Appalachian Mountains, and found that the phenomenon occurs year round (Fig. 1.16). Closer inspection of the data, however, reveals a seasonal signature in the frequency of occurrence, with 67% of all damming events and 68% of all damming days taking place from October to April (Bell and Bosart 1988). The tendency for CAD to occur during the cold season is similar to the seasonality observed with respect to MHC.

A case study of the CAD event of 21–23 March 1985 presented by Bell and Bosart (1988) also presents a conceptual model of how CAD develops along the eastern slopes of the Appalachians (Fig. 1.17). Prior to this damming event, Bell and Bosart (1988) note "classic precursor conditions" (not shown), including the relative positions of two 500 hPa troughs. The subsidence which results from the passage of the first 500-hPa trough is able to drive a surface anticyclone into the region (following the passage of a surface cold front) well before the arrival of a surface cyclone associated with the second, southern 500-hPa trough. In this way, down-gradient surface flow is able to drive cold air southward along the eastern slopes of the Appalachians before the southern trough can induce coastal surface cyclogenesis and its associated warm-air advection (Bell and Bosart 1998). The notion of an identifiable synoptic-scale pattern heralding the onset of a mesoscale phenomenon will be shown to be applicable to cases of MHC as well.

As synoptic-scale warm-air advection (WAA) at 850 hPa begins in the region and cold-air advection (CAA) at the surface continues, Bell and Bosart (1988) indicate the development and eventual strengthening of a sloping inversion at the top of the surface cold pool. In this fashion, a positive-feedback mechanism ensues, in which the strengthening inversion renders the cold pool increasingly stable. This mechanism differs fundamentally from the processes that drive MHC, which occurs within an inherently transient synoptic regime. Conversely, the shallowness of CAD and its attendant dome of low-level cold air, which Bell and Bosart (1988) indicate develops below 850 hPa and is therefore not evident on mandatory-level constant pressure charts, is similar to the shallow nature of MHC, which, too, is not directly evident on such charts. Indeed, CAD is most readily apparent from the surface to 930 hPa, a level at which Bell and Bosart (1988) indicate that winds are "clearly orographically influenced," as evidenced by a substantial northeasterly bias in wind direction as compared to overlying flow. The winds at the 930-hPa level (with speeds ranging from 12 to 17 m s^{-1}) are referred to by Bell and Bosart (1988) as the low-level wind maximum (LLWM), which the authors state is accelerated by an unbalanced along-mountain component of the pressure-gradient force. Air flowing toward the mountains is partially blocked and slows down, resulting in a weakening of the Coriolis force and the creation of an unbalanced pressure gradient force with resulting down-gradient mountain-parallel flow. The CAD signature weakens when the mountain-parallel component of the low-level flow decreases, allowing the cold dome to disperse and expand toward the coast. The CAD signature is eliminated when the mountain-perpendicular component of the flow becomes directed away from the mountains. Thus, while low-level wind speeds and pressure gradients exceed those seen in cases of MHC (see Table I), both CAD and MHC are pressure-gradient-driven channeling phenomena.

1.2.2.6 Saint Lawrence River Valley

Close to the Mohawk and Hudson River valleys of eastern New York State is the St. Lawrence River valley, shown in Fig. 1.1b as the broad area of low elevation that emanates northeastward from the eastern shores of Lake Ontario. Roebber and Gyakum (2003) discuss the role that the St. Lawrence valley played in the development of a long-duration catastrophic ice storm that brought more than 100 mm of freezing rain to parts of northern New York and New England in the United States, and Quebec, Ontario, and New Brunswick in Canada from 5–9 January 1998. This icing event developed under the influence of a strong high pressure system situated off the eastern seaboard of the United States (a Bermuda high), which delivered moisture-rich air (PWAT values 2.5 times greater than the climatological average) and light-to-moderate rains to the region concurrent with the arrival of shallow, low-level cold air. This cold air was initially introduced by the passage of a surface cold front, and an extended period of cold surface flow into the region ensued as a strong surface high developed over north-central Quebec. Five analogous events, occurring over a 34 year period, were examined by Roebber and Gyakum (2003), who indicate that even "the best analog produced maximum precipitation amounts less than 50% of the 1998 event."

Pointing to surface wind observations from Montreal and Ottawa (not shown) as evidence of pressure-driven channeling within the St. Lawrence Valley, Roebber and Gyakum (2003) hypothesize that this effect was "crucial" in determining the type of precipitation at times during the event. Fig. 7 (not shown) from Roebber and Gyakum (2003) also provides evidence of orographic flow channeling based on data collected by the McGill University wind profiler (located in Montreal), showing a discontinuity between near-surface winds (easterlies and northeasterlies) and overlying winds (southwesterlies). While more pronounced in the case of the 1998 ice storm, low-level wind signatures which are decoupled from the overlying synoptic-scale flow are also evident in cases of MHC.

Roebber and Gyakum (2003) attribute maximum precipitation amounts from the 1998 ice storm to the presence of a deformation zone in the vicinity of the St. Lawrence Valley and frontogenetical forcing. Frontogenesis was locally enhanced by persistent down-valley transport of cold air driven by pressure-gradient-driven flow channeling, which had the effect of controlling not only precipitation intensity (an effect also seen in cases of MHC), but also precipitation type in the region. Indeed, model (MM5) simulations conducted by Roebber and Gyakum (2003; not shown) indicate that little or no freezing rain would have occurred at Burlington, Vermont, had flow channeling not occurred. Pressure-gradient-driven channeling, responsible for keeping the surface-based freezing line from retreating northward despite the surrounding synoptic-scale conditions, was found by Roebber and Gyakum (2003) to play a vital role in sustaining the long-duration icing event. The inherent difficulty in forecasting mesoscale features prevented forecasters at the time of this event from properly identifying its magnitude; however, as the presence and effect of orographic channeling is tied to the synoptic-scale pressure field, Roebber and Gyakum (2003) "speculate that the intrinsic predictability of such events may be relatively high."

1.2.3 Effects of the Mohawk and Hudson River Valleys on Overlying Synoptic Flows

Several previous studies have examined the impacts of complex terrain on the weather of eastern New York and western New England. As of this writing, there are no existing references in the refereed literature on how the Mohawk and Hudson valleys may influence cold season weather regimes in the region. There are, however, recent refereed publications that address the influence of these valleys on warm-season severe weather within the region, including Wasula et al. (2002), LaPenta et al. (2005), and Bosart et al. (2006). Reviews of these publications follow, in an effort to assess the flow-channeling properties of the Mohawk and Hudson valleys.

Wasula et al. (2002) addressed the climatology of severe weather (wind, hail and tornado reports) over eastern New York and western New England in relation to terrain influences (for an overview of the terrain, see Figs. 1.1d, 1.2). Surface wind roses were generated for hourly observations of wind direction between March 1993 and March 1997 at Albany, NY (ALB), and from July 1995 through May 1997 at Utica, NY (UCA). These wind roses are presented in Fig. 1.18, showing a tri- and bimodal wind distribution at ALB and UCA, respectively. At ALB, the three dominant wind directions (in terms of frequency of occurrence) are south, north, and west-northwest, and at UCA are west-northwest and east-southeast. Noting that these wind directions at ALB (UCA) align well with the axes of the Mohawk and Hudson (Mohawk) River valleys, Wasula et al. (2002) conclude that "near and just above the surface the terrain funneling is an important effect." Additional wind roses (not shown), constructed from atmospheric sounding data at 850, 700, and 500 hPa, indicate an increased tendency for severe weather reports to occur south of the Mohawk Valley into the Catskills and Berkshires on severe weather days with northwest flow, and a preference for severe weather reports to occur from the Mohawk valley northward into the southern Adirondacks on southwest-flow severe weather days.

LaPenta et al. (2005) present a multiscale examination of the Mechanicville, NY, tornado of 31 May 1998, finding that the Hudson River valley may have locally enhanced the already favorable tornadic environment present that day. The authors find the presence of southerly near-surface flow within the Hudson valley at the same time south-southwest flow was observed to the west of the valley. Such an in-valley flow may have increased the northward transport of heat and moisture (refer to LaPenta et al. 2005, Fig. 24; not shown).

Bosart et al. (2006) examined how the complex terrain of eastern New York and western New England influenced the development of the 1995 Great Barrington, MA (GBR), tornado and its parent mesocyclone. The authors found a pattern of marked rotational intensification as the mesocyclone moved from the high terrain located west of the Hudson River valley into the valley itself, followed by a marked weakening as the mesocyclone continued eastward over the mountains of western Massachusetts. Bosart et al. (2006) conclude that "the most important factor in the observed intensification of the GBR mesocyclone and ensuing tornadogenesis was the existence of a terrain-channeled low-level (0–1 km) southerly flow in the Hudson [v]alley...." As compared to the background environment, this flow channeling produces a more clockwise-turned hodograph at low levels and lengthens the hodograph (i.e. increases the shear) overall.

1.3 Goals and Thesis Synopsis

The ultimate goal of this research is to determine how the topography of eastern New York and western New England interacts with overlying synoptic-scale conditions to generate a zone of low-level convergence and mesoscale precipitation in the vicinity of Albany, NY. Building on previous research which shows the Mohawk and Hudson River valleys to be effective agents for channeling of low-level flow (i.e., Wasula et al. 2002;

LaPenta et al. 2005; and Bosart et al. 2006), the impacts on MHC of pressure-gradient-driven channeling in these valleys will be addressed in this study.

In an effort to determine empirically the processes that drive MHC, several case studies were completed. Two such cases (27 November 2002 and 29 January 2007) are considered "benchmark" cases, and are presented in greater detail. Four other cases (16–17 December 2002, 23 January 2003, 17 January 2005, and 3 March 2006) are presented as supporting cases and are described in lesser detail. These cases were analyzed individually and in the aggregate to determine similarities and differences between them. A seventh case of interest occurred on 2 January 2008, just prior to the completion of this thesis. Sufficient time was not available to undertake an in-depth analysis of the January 2008 event, but an overview of it is included here for completeness.

The physical processes necessary to generate a MHC event will be discussed, including positive north–south (west–east) SLP differences along the Hudson (Mohawk) valley that drive the convergent flow, an absence of strong CAA, which precludes strong subsidence and drying of the boundary layer, and statically stable atmospheric stratification, which prevents downward momentum transfer that could damp out the convergent wind signature. A discussion of the synoptic-scale features that contribute to the aforementioned mesoscale environment will also be presented.

Finally, an effort is made to increase the predictive skill of future MHC events through the use of an operational forecasting scheme. To this end, a conceptual model detailing the interplay during MHC events of upper-air and surface weather features and orography is presented, and a decision tree for forecasters is developed.

1.4 Organization of the Thesis

Chapter 2 addresses the acquisition of observational and model data sources used to develop MHC case studies. The parameters used to describe and those used to make comparisons between each case study comprises an explanation of methodology. Statistical results of these comparisons and an objective analysis and description of each of the seven case studies are presented in Chapter 3. Chapter 4 contains an overview of the findings gained from the case studies, which will be presented in light of the reviewed literature and also with respect to MHC formation and forecasting. A conceptual model of MHC and a decision tree to aid in operational forecasting of this phenomenon also is presented in Chapter 4. Lastly, Chapter 5 includes the conclusion of this thesis as well as suggested avenues of exploration for future researchers.

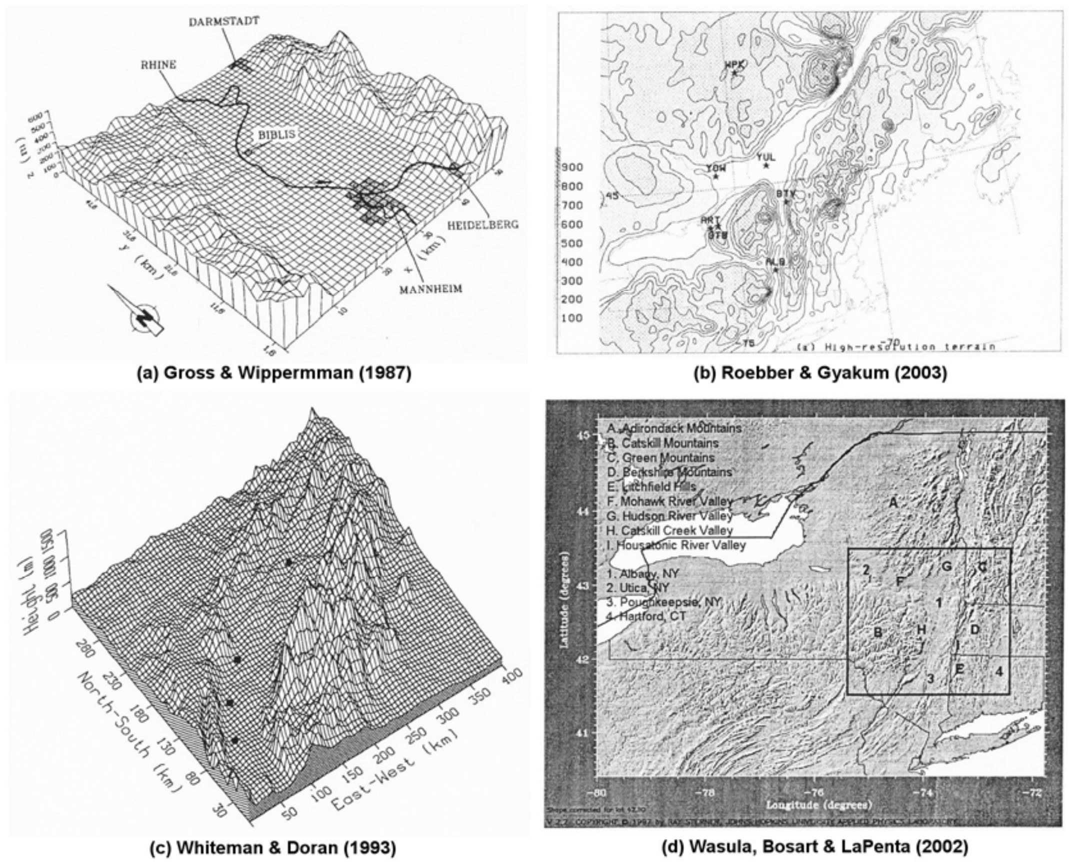

Figure 1.1: Topographic features of selected flow-channeling case studies. (a) The northern part of the upper Rhine valley. (Source: Fig. 2 from Gross and Wippermann 1987). (b) Fifth-generation Pennsylvania State University–National Center for Atmospheric Research Mesoscale Model (PSU–NCAR MM5) 9 km resolution topography (contours and shading) of the northeastern U.S. and southeastern Canada. Contour interval is 100 m, beginning at 100 m, with progressively darker shading for higher elevations. (Source: Fig. 2a from Roebber and Gyakum 2003). (c) Topography of the Tennessee Valley, with the locations of four observation towers indicated. (Source: Fig. 2 from Whiteman and Doran 1993). (d) Terrain map of New York and New England with important terrain and political features labeled. (Source: Fig. 1 from Wasula et al. 2002).

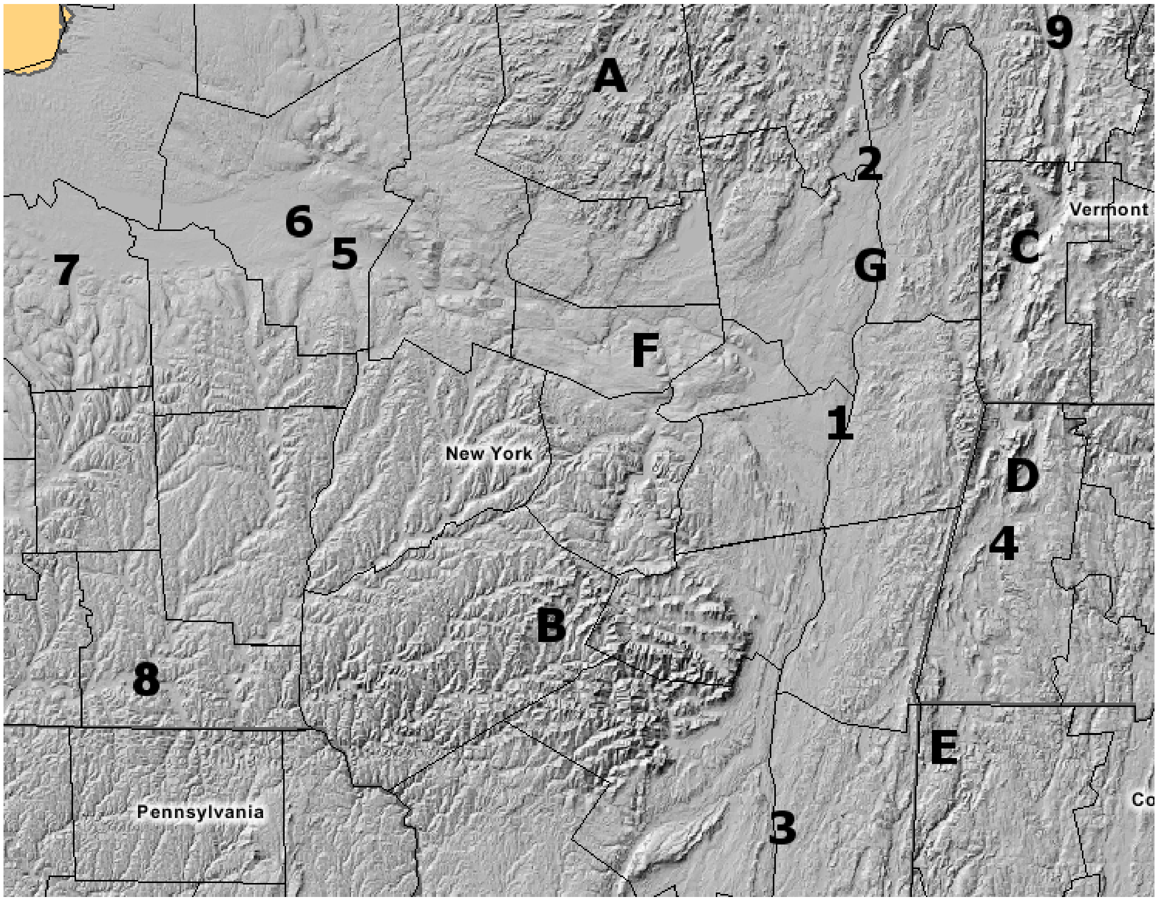

Figure 1.2: Terrain map of Mohawk–Hudson Convergence (MHC) domain in New York and western New England, with important terrain and political features labeled: (1) Albany, NY (KALB), (2) Glens Falls, NY (KGFL), (3) Poughkeepsie, NY (KPOU), (4) Pittsfield, MA (KPSF), (5) Utica, NY (KUCA), (6) Rome, NY (KRME), (7) Syracuse, NY (KSYR), (8) Binghamton, NY (KBGM), (9) Rutland, VT (KRUT), (A) Adirondack Mountains, (B) Catskill Mountains, (C) Green Mountains, (D) Berkshire Mountains, (E) Litchfield Hills, (F) Mohawk River valley, (G) Hudson River valley.

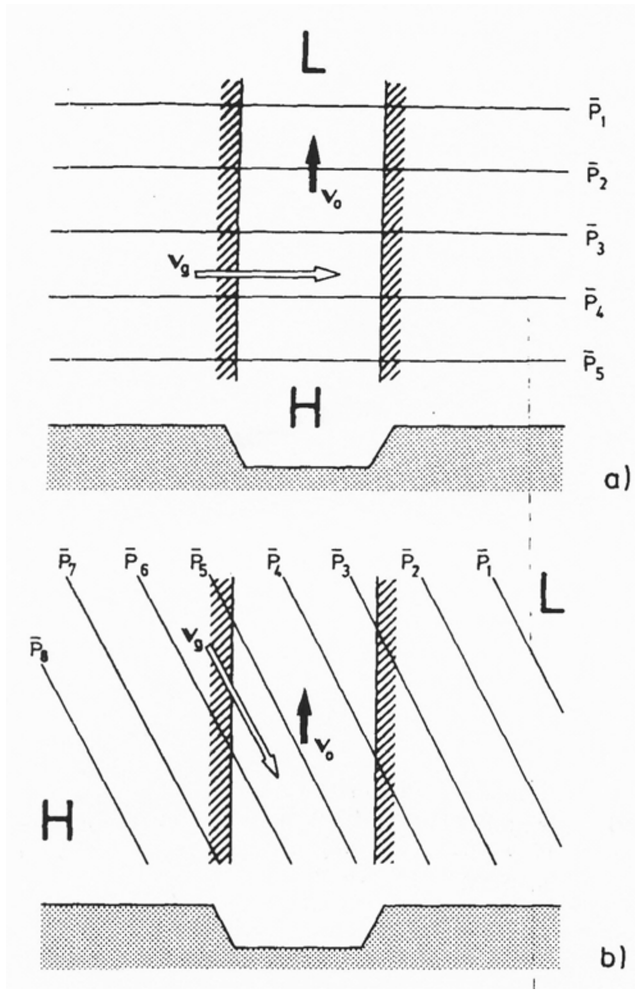

Figure 1.3: Schematic from Gross and Wippermann (1987; originally Fig. 1) showing channeling (**v**, black arrow) for (a) a geostrophic wind perpendicular to the valley, above, and (b) a counter-current, below.

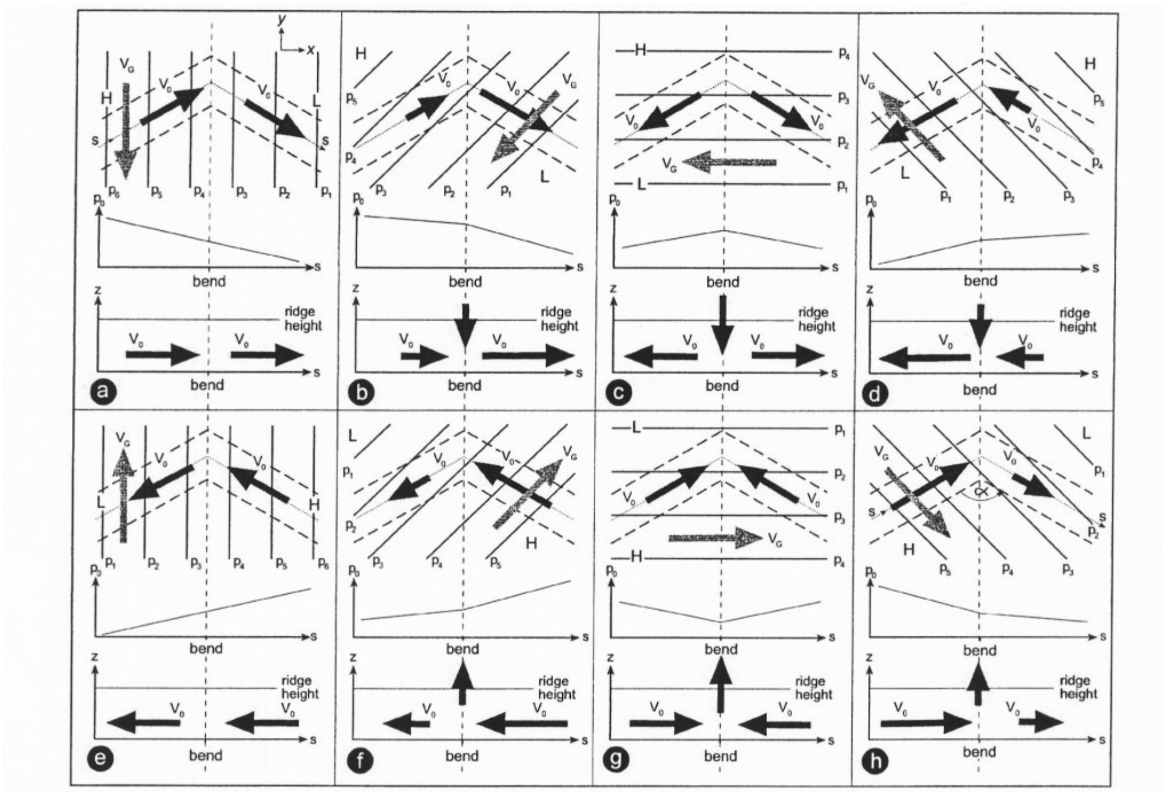

Figure 1.4: Plan and cross-section representations of pressure-driven channeling in a bent valley from Kossman and Sturman (2003; originally Fig. 3). Here, the angle formed by the valley bend (α) is 120°, with geostrophic wind directions from (a) north, (b) northeast, (c) east, (d) southeast, (e) south, (f) southwest, (g) west, (h) northwest; *s* indicates the along-valley direction. For Mohawk-Hudson convergence, α equals approximately 100°, and schematic (h) most closely represents the attendant synoptic conditions.

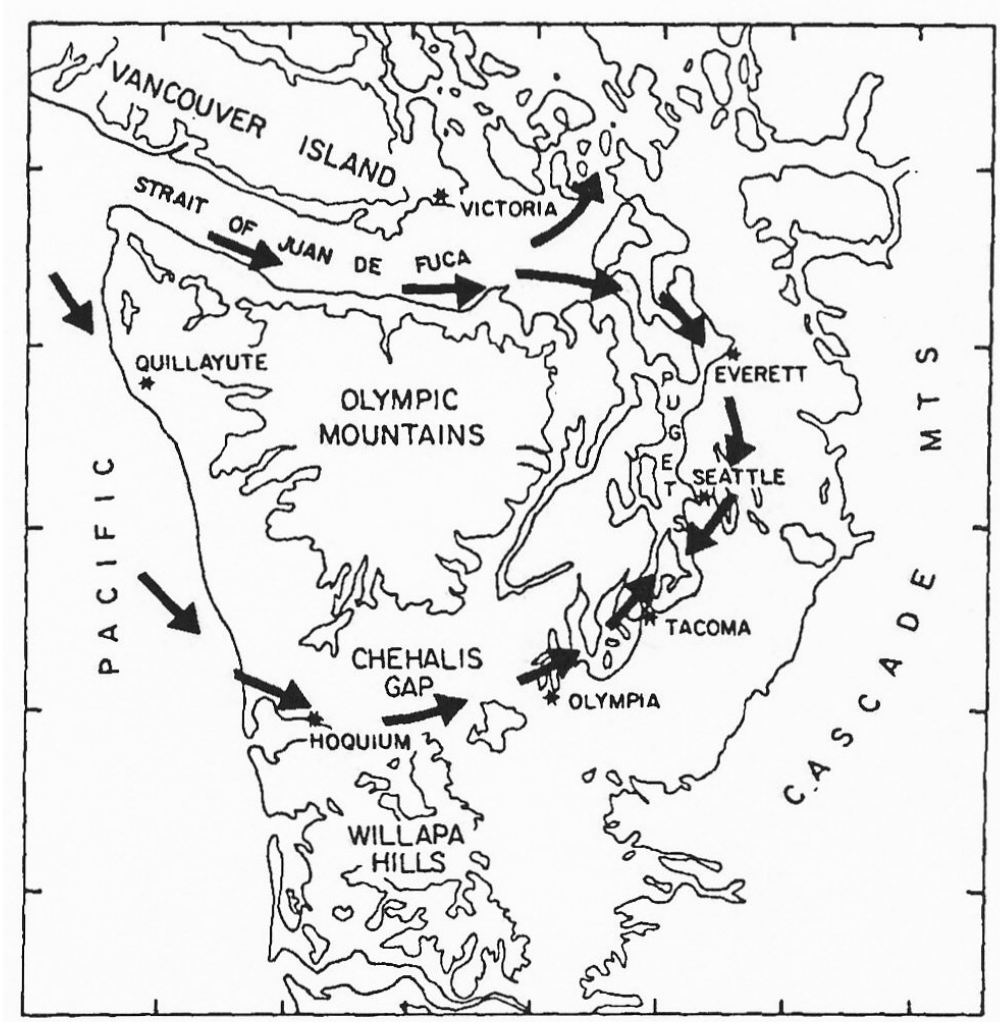

Figure 1.5: Major cities and geographical features of western Washington State. Thin, solid lines indicate elevation, every 300 m. The arrows represent typical surface winds during a Puget Sound convergence event. (Source: Fig. 2 from Mass 1981).

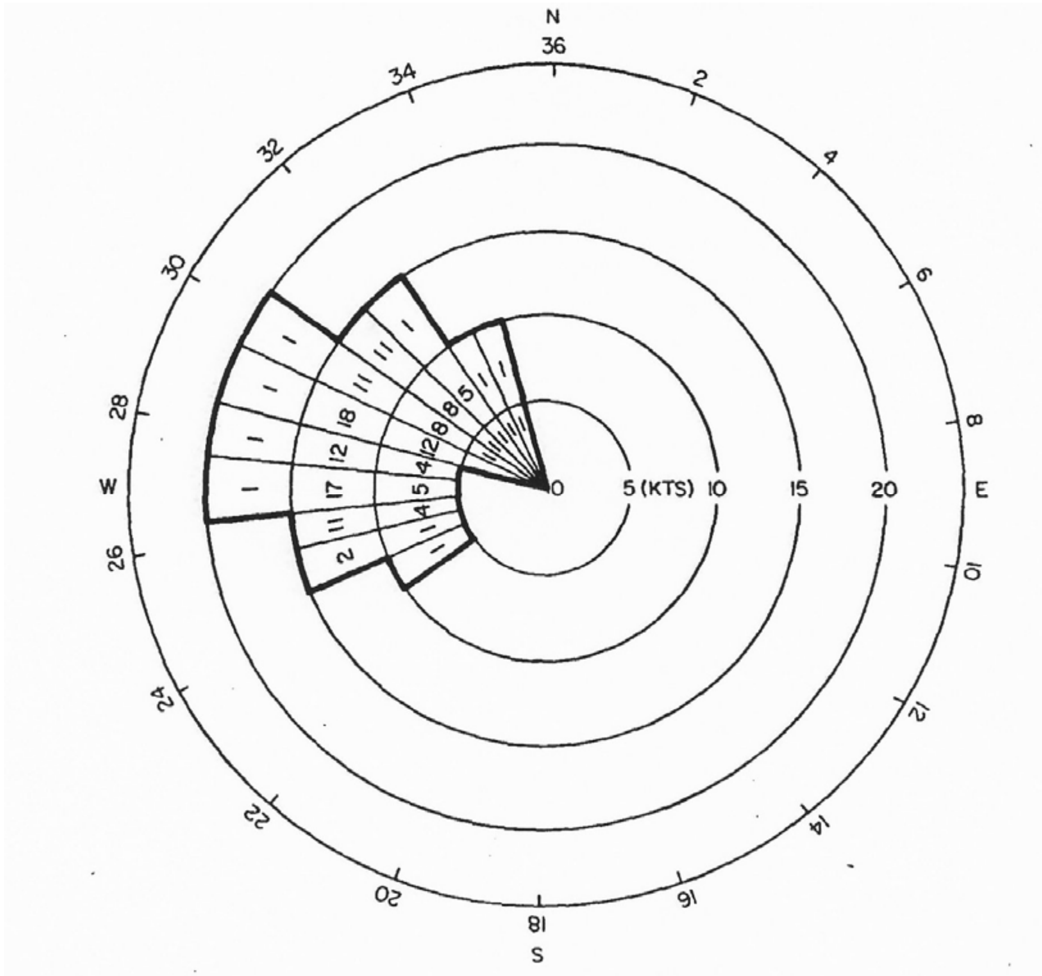

Figure 1.6: Polar representation of the surface wind speed and direction at Hoquium, Washington (KHQM), during 10 Puget Sound convergence events. (Source: Fig. 4 from Mass 1981).

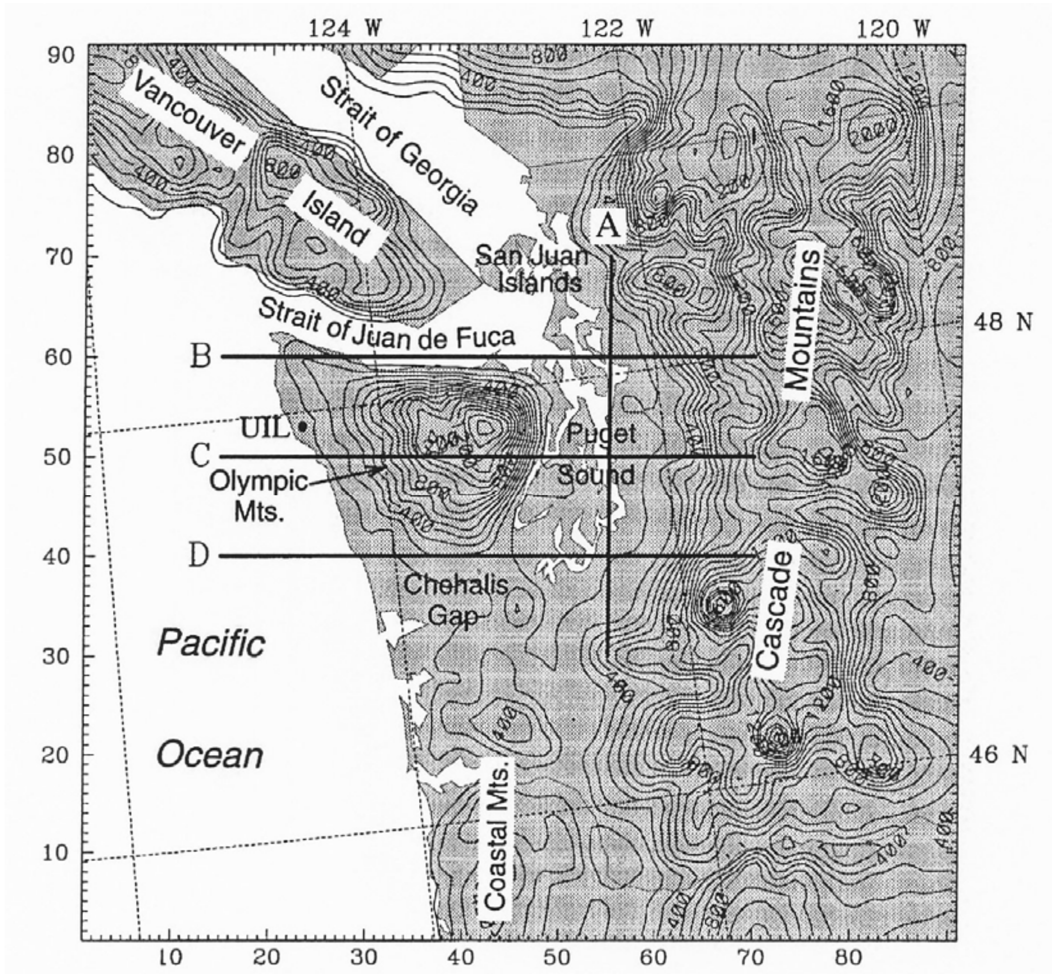

Figure 1.7: Terrain height (contour interval of 100 m) for the control experiment using a PSU–NCAR MM5 model simulation. The heavy black lines (labeled A–D) indicate the position of cross sections that are referenced in section 1.2.2.1. (Source: Fig. 1 from Chien and Mass 1997.

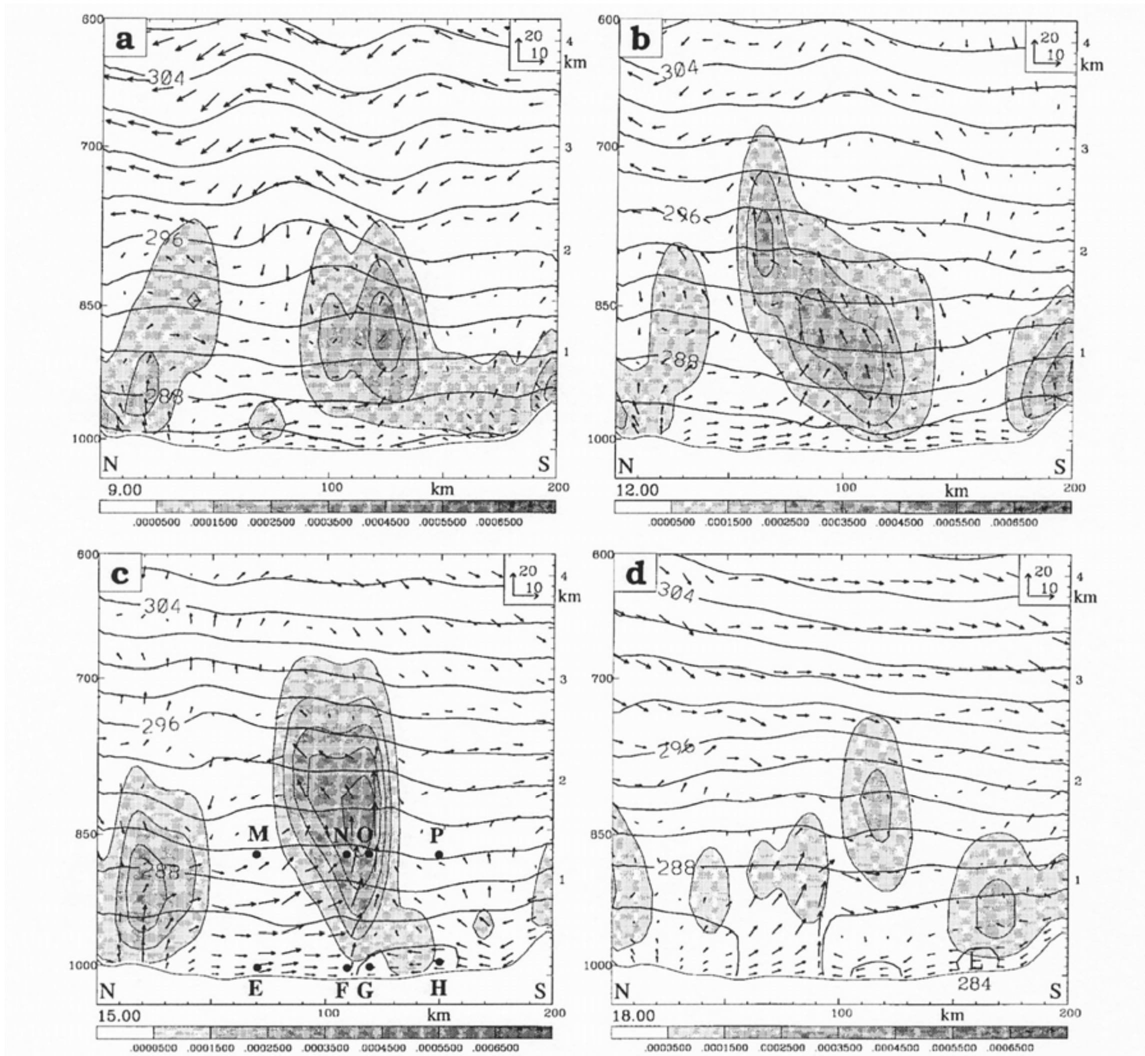

Figure 1.8: North–south cross sections along line A in Fig. 1.7 at (a) 0900, (b) 1200, (c) 1500, and (d) 1800 UTC 26 May 1992 for the control simulation. Thick solid lines are isentropes at a 2-K interval. Wind vectors represent flow within the cross section. Wind vector scales are shown at the upper-right corner of each plot (horizontal wind, m s^{-1}; vertical velocity, μb s^{-1}). Shaded areas denote cloud water mixing ratio. (Source: Fig. 6 from Chien and Mass 1997).

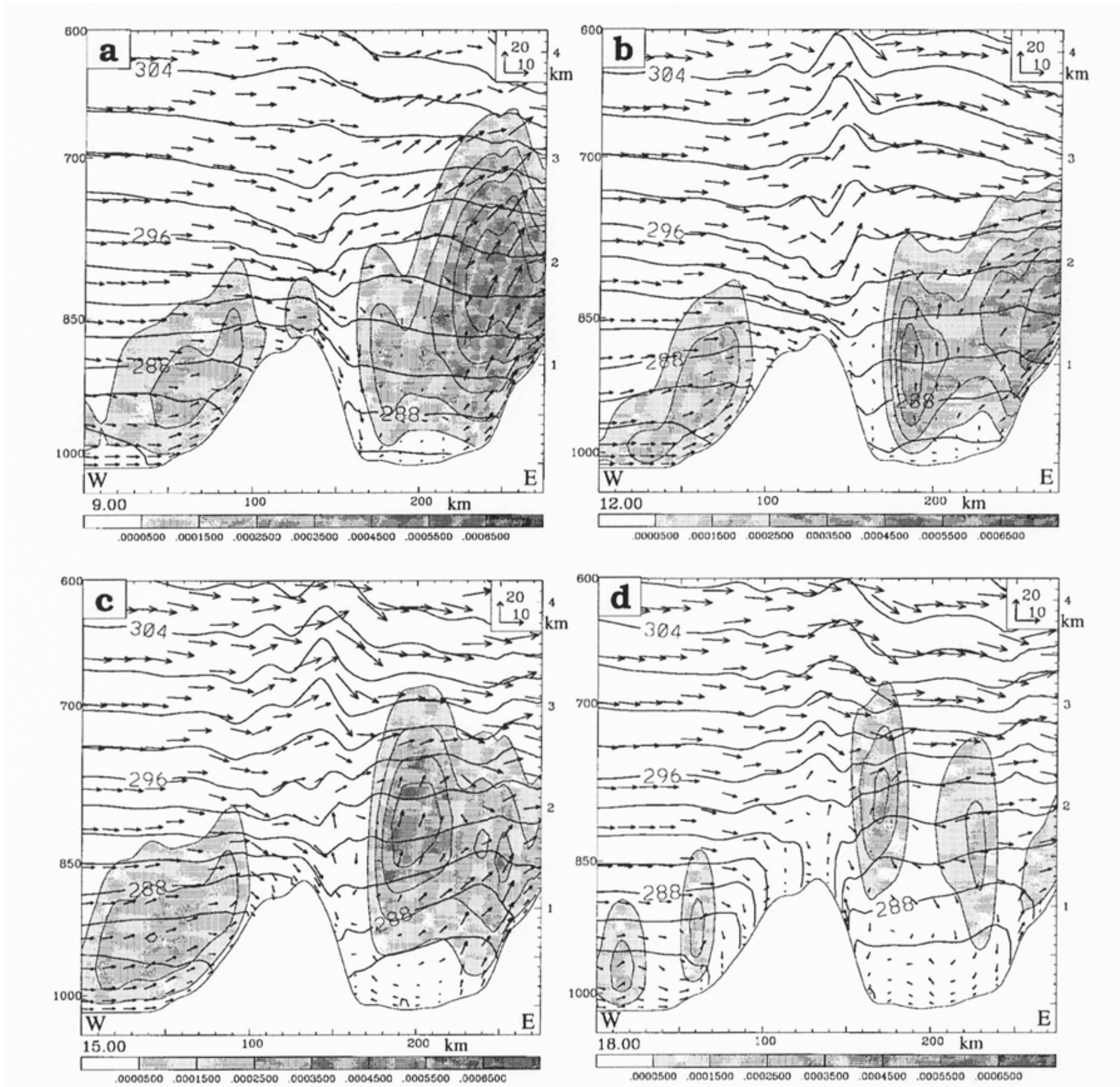

Figure 1.9: West–east cross sections along line C in Fig. 1.7 at (a) 0900, (b) 1200, (c) 1500, and (d) 1800 UTC 26 May 1992. Presented fields and contour conventions are the same as for Fig. 1.8. (Source: Fig. 7 from Chien and Mass 1997).

Month	Number of CZ events	Number of predicted CZ events	Number of correct predictions
January	0	3	0
February	2	3	2
April	9	11	9
May	12	13	11
Total	23	30	22

Figure 1.10: Results of an experiment to determine the feasibility of forecasting [Puget Sound] convergence zone (CZ) events. (Source: Table 1 from Mass 1981).

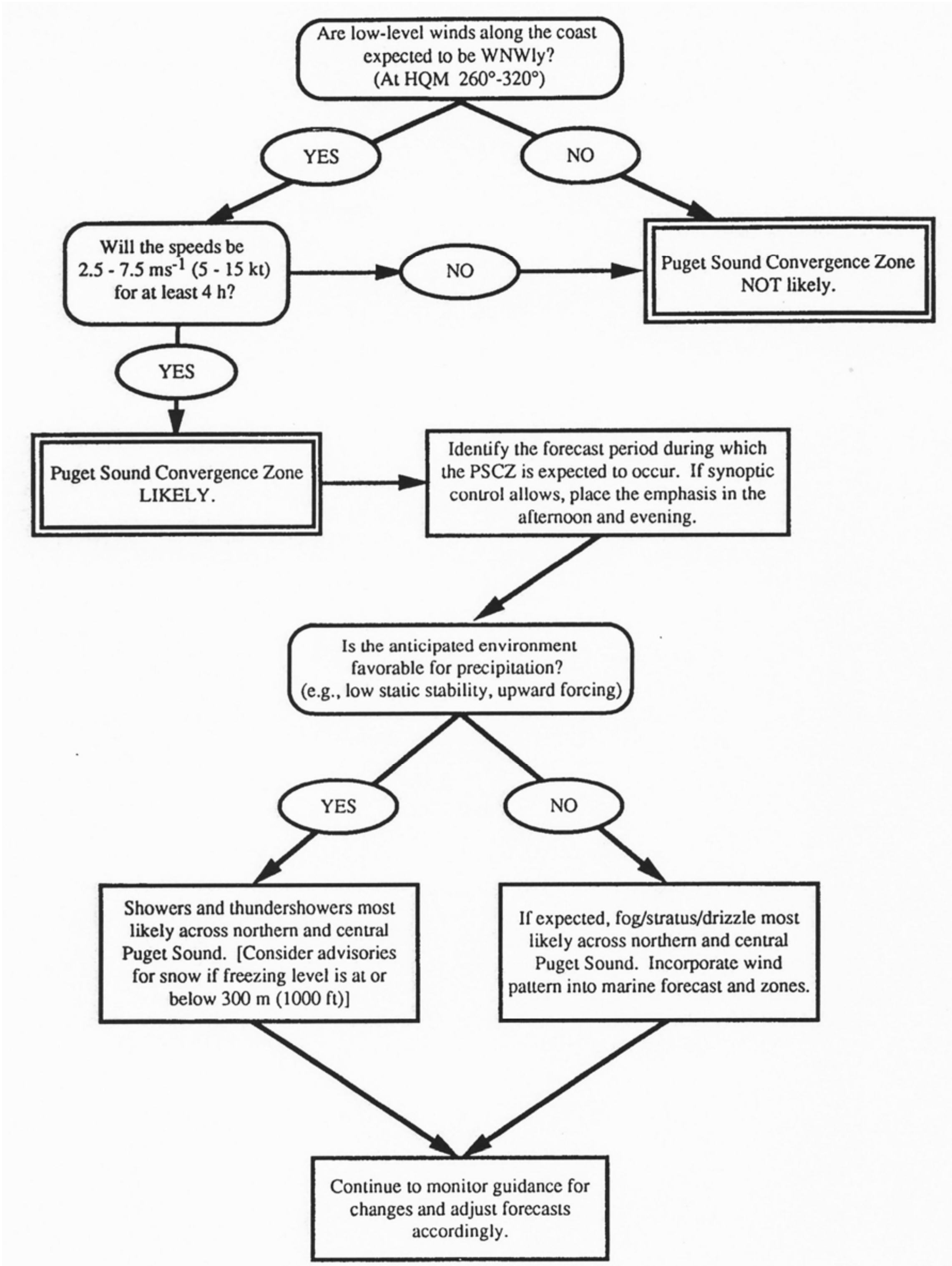

Figure 1.11: Decision tree for forecasting the Puget Sound convergence (PSCZ). (Source: Fig. 2 from Whitney et al. 1993).

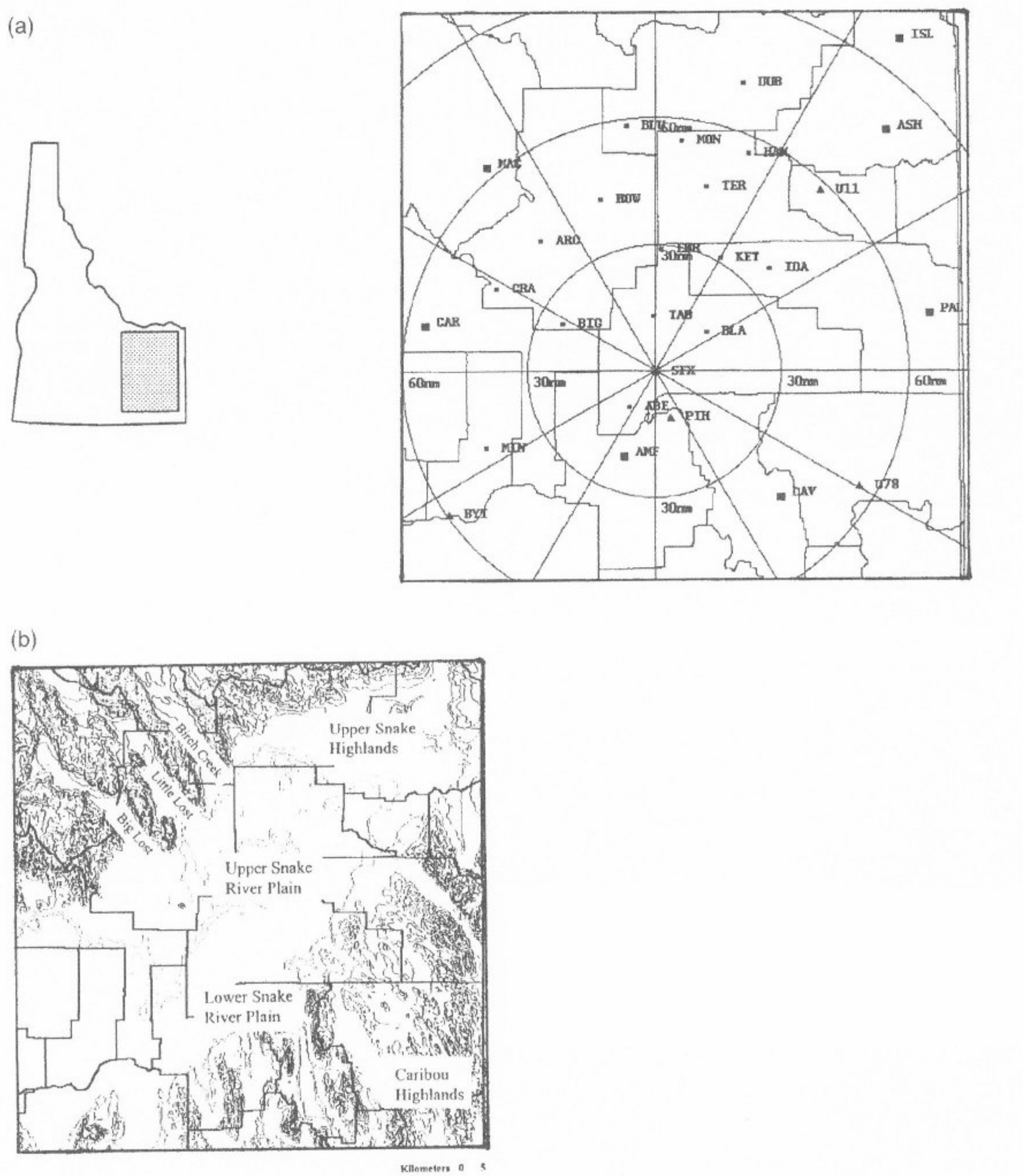

Figure 1.12: (a) Important political features of eastern Idaho, showing the location of mesonet sites (small squares), NWS METAR stations (triangles), city locations (large squares), the Springfield, ID (SFX), Weather Surveillance Radar–1988 Doppler (WSR-88D) (diamond) and range rings (nautical miles). (b) Topographic map of eastern Idaho and geographical references. (Source: Fig. 1 from Andretta and Hazen 1998).

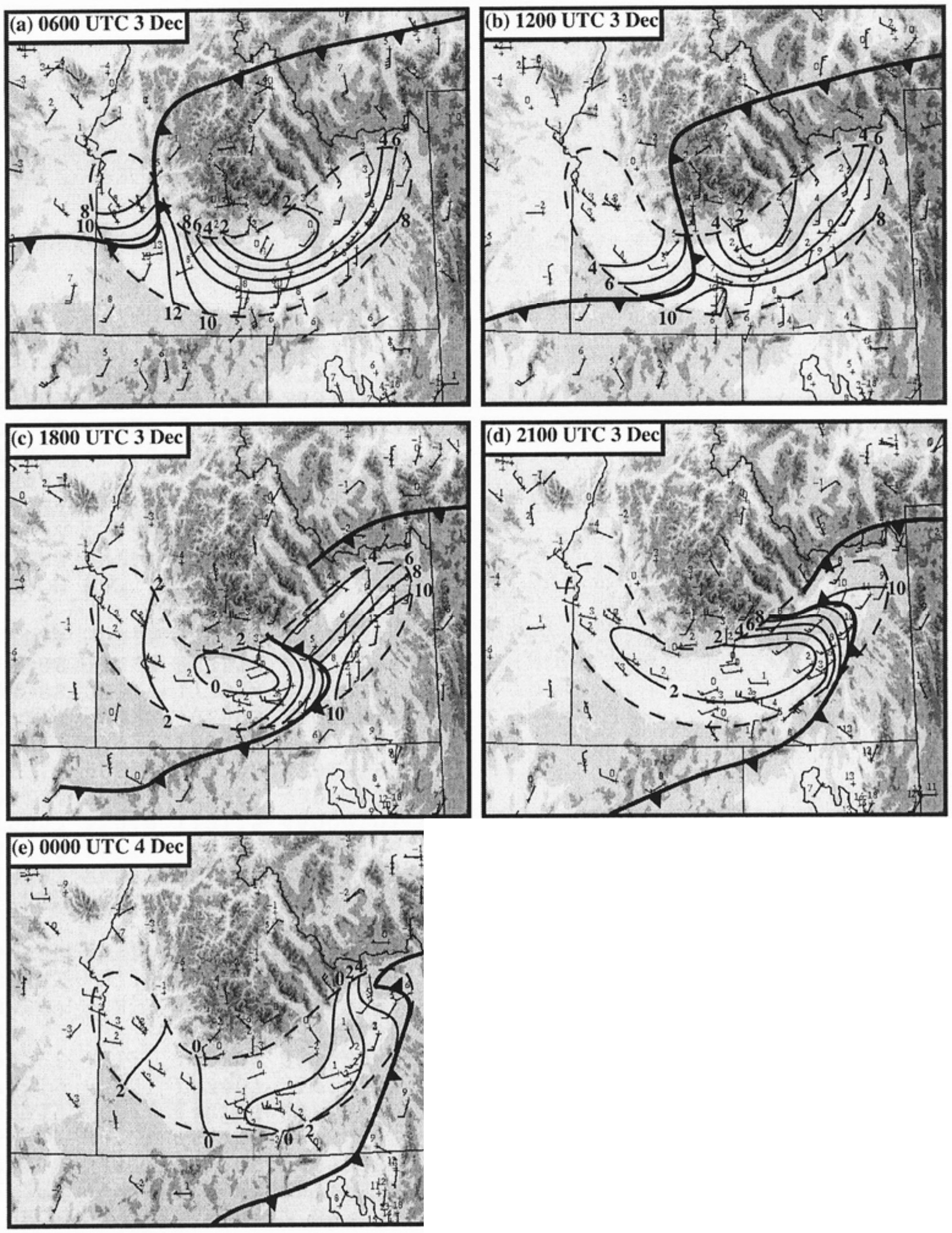

Figure 1.13: Mesoscale frontal analyses (conventional frontal symbols) and low-level isotherms (every 2°C) within the region identified by a dashed line (the Snake River Plain of Idaho) at (a) 0600 UTC 3 Dec, (b) 1200 UTC 3 Dec, (c) 1800 UTC 3 Dec, (d) 2100 UTC 3 Dec, and (e) 0000 UTC 4 Dec 1988. Station plots of wind (full and half barb denote 5 and 2.5 m s^{-1}, respectively) and temperature (°C, upper left). Shading corresponds to terrain. (Source: Fig. 7 from Steenburgh and Blazek 2001).

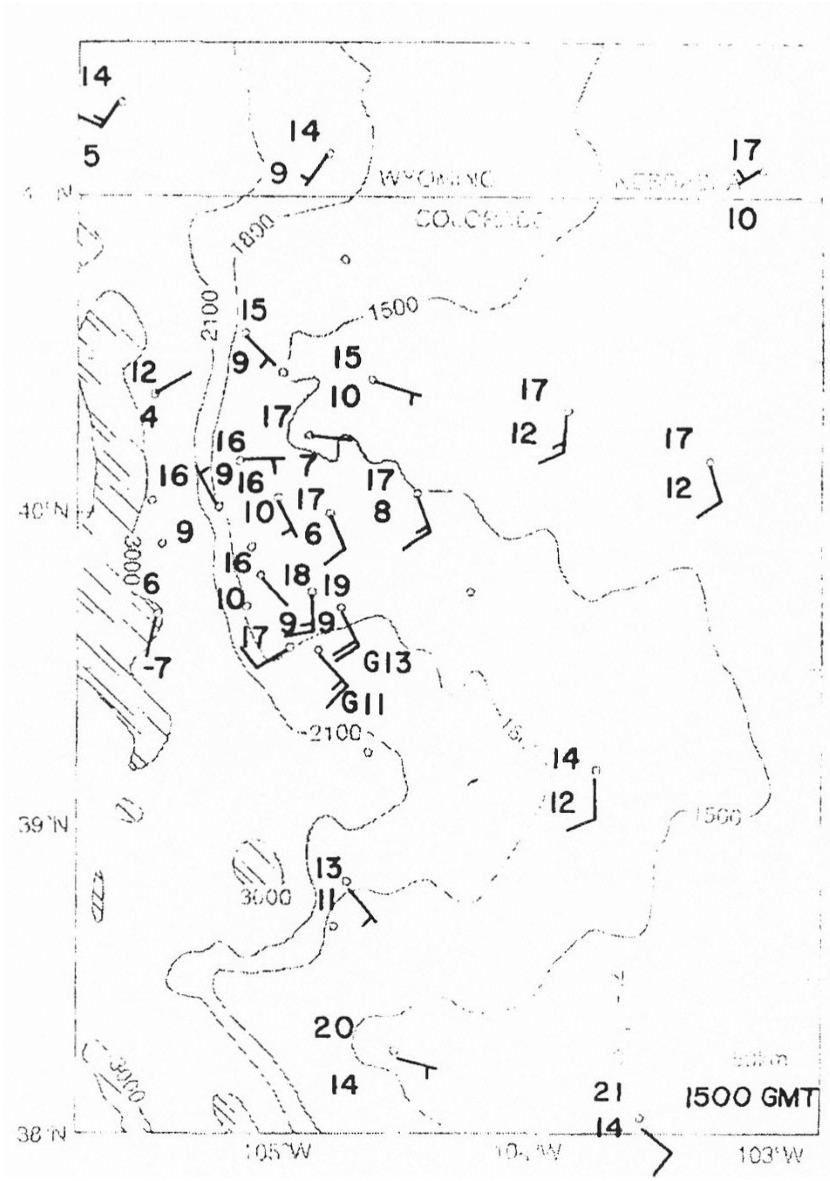

Figure 1.14: Surface plot at 1500 UTC 3 June 1981 of winds associated with the Denver convergence–vorticity zone. Temperature and dewpoint are in °C, full wind barb is 5 m s^{-1}, and G indicates gust speeds in m s^{-1}. Map background shows contours (m) of elevation (hatched above 3000 m). (Source: Fig. 7 from Szoke et al. 1984).

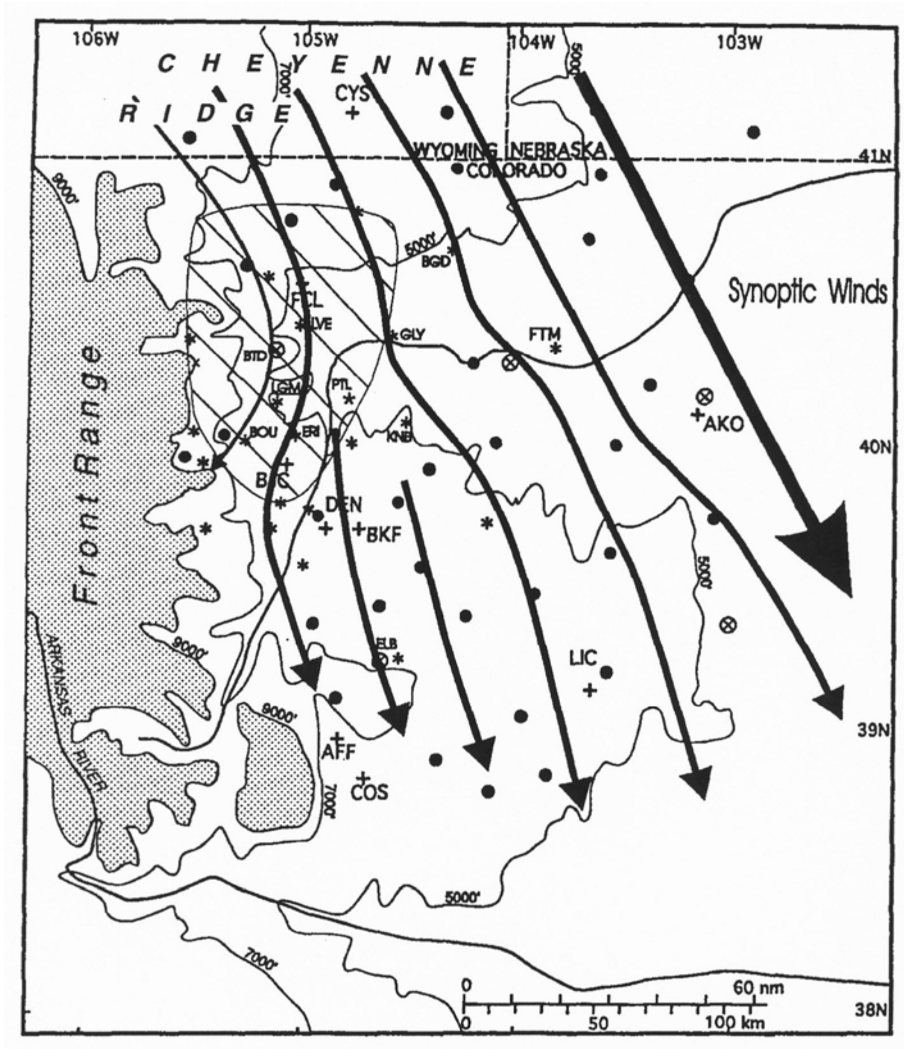

Figure 1.15: Schematic of the general low-level wind flow present during the Longmont anticyclone (LA) event of 16 January 1991. Solid contours indicate elevation, and shading indicates elevations above 2.75 km. Hatching indicates the region of anticyclonic turning and convergence. Several observation sites are labeled with their three-letter identifiers, including CYS: Cheyenne; FCL: Fort Collins; DEN: Denver; COS: Colorado Springs; LIC: Limon; BOU: Boulder; LGM: Longmont. (Source: Fig. 1 from Wesley et al. 1995).

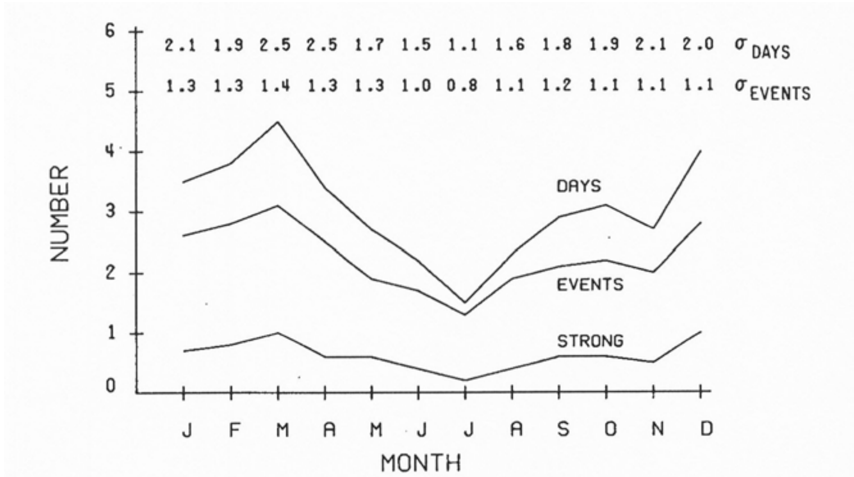

Figure 1.16: A monthly cold-air damming climatology for the eastern Appalachian Mountains spanning 50 years of data. The mean number of actual events is shown by the middle curve. The mean number of days per month in which the eastern Appalachian region is under the influence of damming episodes is shown by the top curve. The mean monthly number of strong damming events is shown by the bottom curve. The bottom (top) horizontal set of numbers above the climatology curves indicates the monthly standard deviation of the number of damming events (the number of days in which eastern Appalachian region is under the influence of damming episodes). (Source: Fig. 3 from Bell and Bosart 1988).

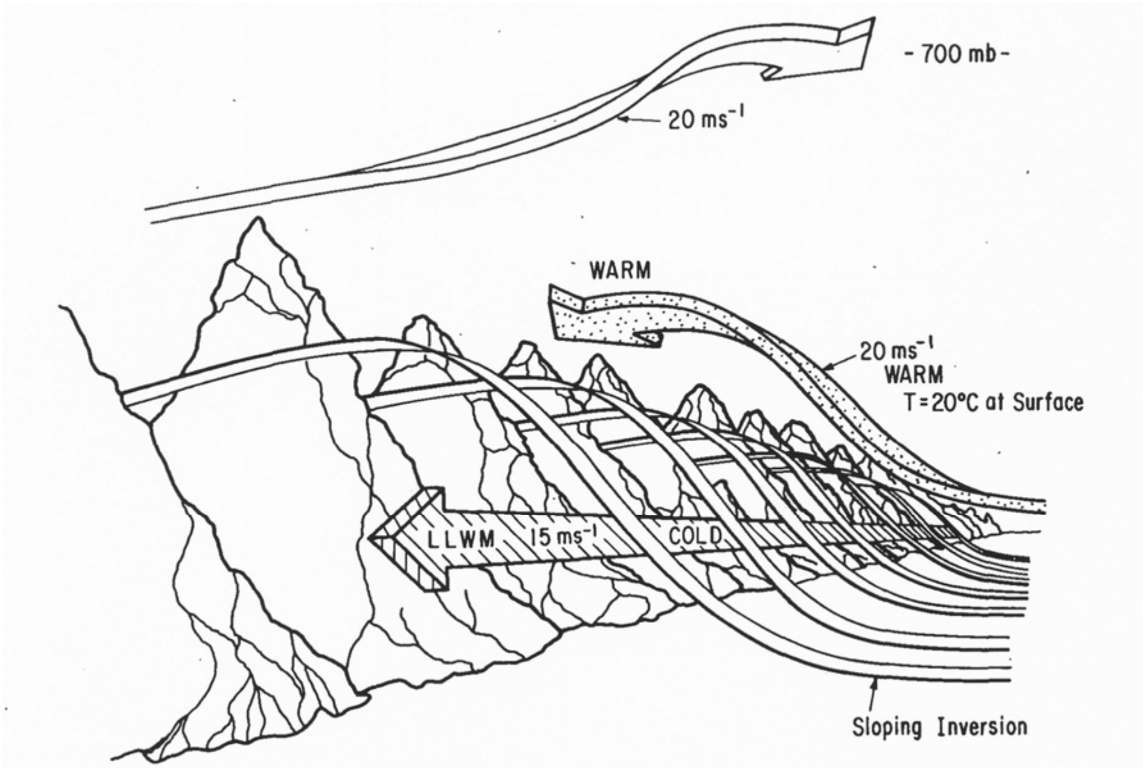

Figure 1.17: Conceptual model of cold-air damming (CAD) as it existed at 1200 UTC 22 March 1985. Note the strong low-level wind maximum (LLWM) within the cold dome, the easterly (or southeasterly) flow just above the cold dome associated with strong warm advection into the warm air above the dome, the sloping inversion of the cold dome top, and the southerly and southwesterly winds above 700 hPa associated with the advancing short-wave trough west of the Appalachian Mountains. (Source: Fig. 22 from Bell and Bosart 1988).

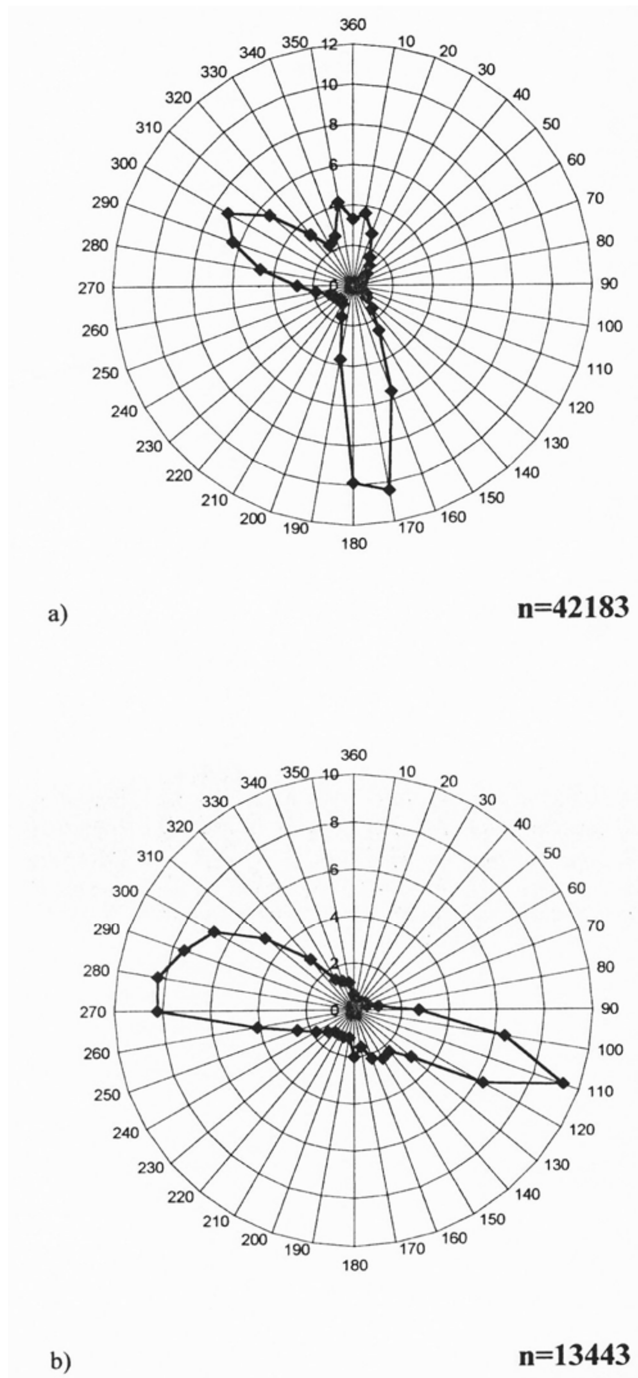

Figure 1.18: Surface wind roses for (a) ALB and (b) UCA for March 1993–March 1997 and July 1995–May 1997, respectively. Azimuthal axis represents wind direction (°), and radial axis represents wind speed (m s^{-1}). (Source: Fig. 4 from Wasula et al. 2002).